

Weather radar refractivity variability in the boundary layer of the atmosphere.

Ruben Hallali¹, Jacques Parent du Châtelet¹, Francis Dalaudier², Gilles Guillemin³, Alain Moreau³

1 Météo-France/ LATMOS Guyancourt, France

ruben.hallali@latmos.ipsl.fr

jacques.parent-du-chatelet@latmos.ipsl.fr

2 LATMOS, IPSL, Guyancourt, France

francis.dalaudier@latmos.ipsl.fr

3 Météo-France

gilles.guillemin@latmos.ipsl.fr

alain.moreau@latmos.ipsl.fr

Weather radars could measure the change in the refractive index of air in the boundary layers of the atmosphere. This technic uses the phase of the signal from ground targets located around weather radars. This measure provides information on atmospheric refractivity which depends on meteorological parameters such as temperature, pressure and humidity. During the HyMeX (Hydrological cycle in Mediterranean Experiment) campaign, refractivity measurements were implemented on several S-band radars of ARAMIS (Application Radar à la Météorologie Infra-Synoptique) French radar network. A study has shown that phase changes have a high temporal variability on both daily and seasonal scales. This variability could be very probably linked to the boundary layer turbulent level. In order to sample temporal and spatial phase variability, an analysis based on a 1-year dataset from S-band and C-band ARAMIS radars and Automatic Weather Stations (AWS) measurements is presented. This inter-comparison, of both radar and AWS measurements, gives a better knowledge of the relationship between the variability of radar refractivity measurements and turbulent level. In further investigations, particular attention will be paid to the phase time derivate and spatial variations during a campaign in controlled conditions. This will help answering the question of recovering boundary-layer turbulent level information from radar refractivity measurements.

1. Introduction

Studies have shown the possibility to measure refractivity (N) with meteorological radar using ground echoes phase variations (Fabry 1997, Fabry et al., 2004). This method was developed for coherent emitters (klystron) and validated during two international campaigns, (IHOP in 2002 and REFRACTT in 2006). A comparison between the radar refractivity retrieval and the discrete points of moisture information from Automatic Weather Stations (AWS) was possible during the campaign. This has shown a very high correlation between radar refractivity retrieval and AWS measurements during long-time periods. Then, the method was adapted and implemented on radar with non-coherent emitters such as those of the operational radar network (Parent du Châtelet, 2008). N measurements lead to near-surface moisture estimation. The lack of skill in convective forecast is related to the fact that current mesoscale models do not fully represent the dynamical structure and the micro-physical process of early convection. One of the conditions to improve forecasts is a better knowledge of the boundary layer moisture field (Pielke, 2001, Sherwood et al., 2010). Refractivity measurements, once implemented on

operational radar network, could be very useful for moisture field measurements in the boundary layer. However, some uncertainties exist, particularly on the local character of the measurements and on the origin of the variability of the signal and consequences of this variability.

Using phase variations data simulation from AWS measurements and real radar phase variations measurements, Besson et al. (2011) has shown that the variability of the signal depends on the period of the day and the year. Seasonal and diurnal dependencies were investigated with a numerical statistical approach. Amplitude of fluctuations is more important during the afternoon than during the night and the same thing is observed also during the summer than during the winter. In order to sample and to characterize this variability, an analysis based on a 1-year dataset from S-band and C-band radars and AWS measurements is presented here. Previous results have suggested that turbulent state of the atmospheric in the boundary layer has a key role in the observed radar signal variability. First, the standard deviation of the refractivity signal from in-situ measurements was calculated. Then, a comparison was done between radar refractivity variability retrieved from known identified ground targets and in-situ refractivity variability from AWS measurements. Finally, an application of Taylors' hypothesis (frozen turbulent structures propagated with the wind) is proved in order to quantify the impact of the spatial integration on the refractivity retrieval by radar.

2. Radar refractivity retrieval:

2.1. Refractivity

The refractivity N is defined as $N = 10^6 * (n - 1)$ with n the refractive index of the atmosphere. Using the work of Bean and Dutton (1966) on the measurements of the thermodynamical constants, N can be written in the form:

$$N = 77.6 * \frac{P}{T} + 3.73 * 10^5 * \frac{e}{T^2}$$

where P is the atmospheric pressure [hPa], T the temperature [K], and e the water vapor pressure [hPa]. There is a direct link between N and the humidity in the atmosphere. As a result, measuring N could give detailed information on the humidity field in the atmosphere.

2.2. Radar refractivity retrieval

In vacuum, the celerity of an electromagnetic wave is c . In the atmosphere, a delay appears due to the refraction phenomenon. The time τ taken by electromagnetic waves to reach a target at range r and return to the radar is:

$$\tau = 2r \frac{n}{c}$$

With n the refractive index. For fixed ground targets, r is a constant and only n varies. Therefore if τ could be measured precisely, the average value of n over the path between the radar and these targets can be determined. Using phase time differences from ground target radar echoes, the delay due to refractivity changes along the beam path can be retrieve if the hypothesis of non-moving targets is done. The phase variations can be computed as follows:

$$\Delta\varphi = \Phi(r, t_1) - \Phi(r, t_0) = \frac{4\pi fr * 10^{-6}}{c} \int_0^r [N(x, t_1) - N(x, t_0)] dx$$

where $\Delta\varphi$ is the phase variations in terms of changes in the refractive index along the beam path between the radar and the target, f is the radar emitter frequency, and r the range of the target. Assuming that an average refractivity value can be calculated along the beam path, the phase variation will be:

$$\Delta\varphi = \varphi(r, t_1) - \varphi(r, t_0) = \frac{4\pi f r * 10^{-6}}{c} * N(t_1) - N(t_0)$$

During the rest of the study, mean values of refractivity along beam path will be calculated from radar data.

3. Data and tools

Two datasets were available for this study: AWS measurements of temperature, moisture, pressure and wind every 6 minutes, and radar measurements from Trappes (East of Paris Fig. 1) and Nîmes (South-East of France) every 5 minutes. The analysis of AWS measurements highlights temporal variability of the signal and permits to define several time periods, depending on the refractivity variability. Three periods are defined:

- Period of strong refractivity variability
- Period of low refractivity variability
- Interim periods of transition between the previous ones.

Interim periods are defined in order to avoid ambiguities during transitions between high atmospheric refractivity variability and low atmospheric refractivity variability (cf. Fig. 3)

Description of the in-situ dataset

Several automatic stations were available in the radars areas (13 around Trappes and 12 around Nîmes). These stations measure temperature at 2m, relative humidity at 2m, pressure, rainfall amounts and also wind strength and direction at 10m. When the pressure is not measured, since spatial variability of this parameter is very low, measurements from a reference station (Trappes and Nîmes in-situ stations) were used.

Description on the radar dataset:

One year of radar data for Trappes and Nîmes is available for the study. Coherent and incoherent energy and phase of the signal are measured by the radar every 5 minutes for the lowest available elevation (0.4° for Trappes and 0.6° for Nîmes). The lobe for these radar is 1° and the range of the gates 240m.

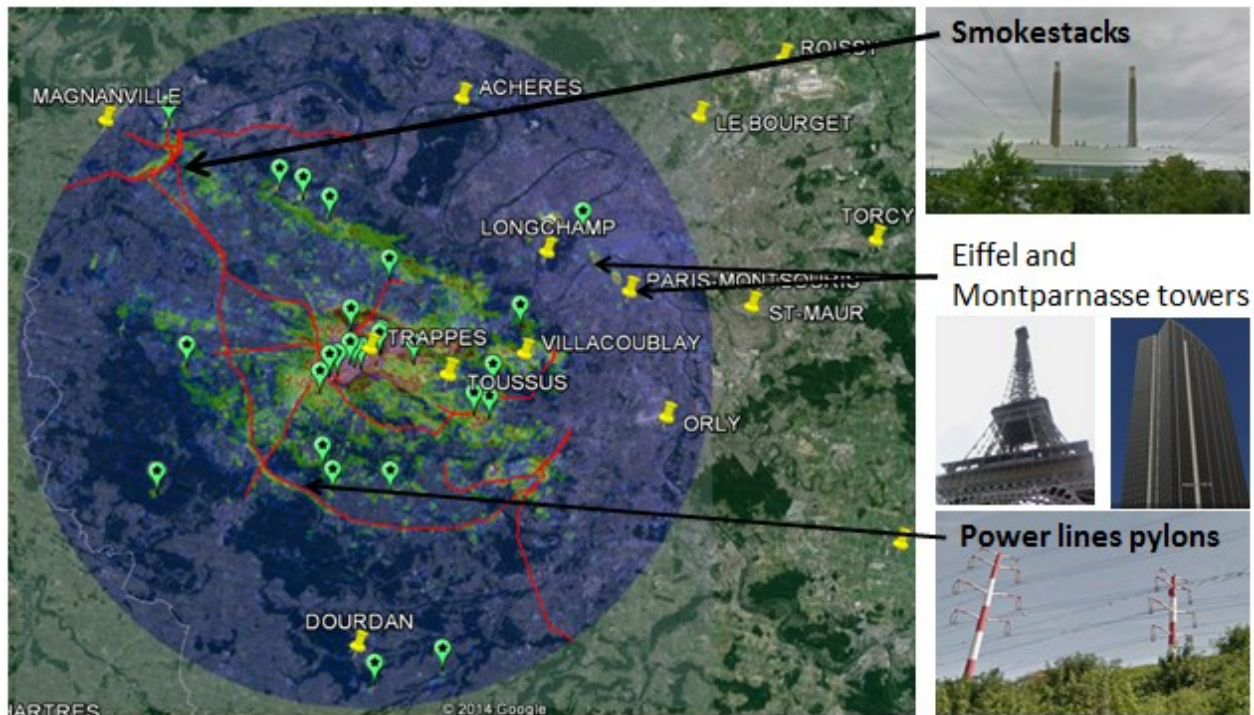


Fig. 1: Reflectivity around Trappes radar at 0.4° elevation angle projected on google maps. Red lines represent power lines. Green points represent other identified ground echoes such as antenna, water tower or buildings. Yellow icons represent Automatic Weather Stations

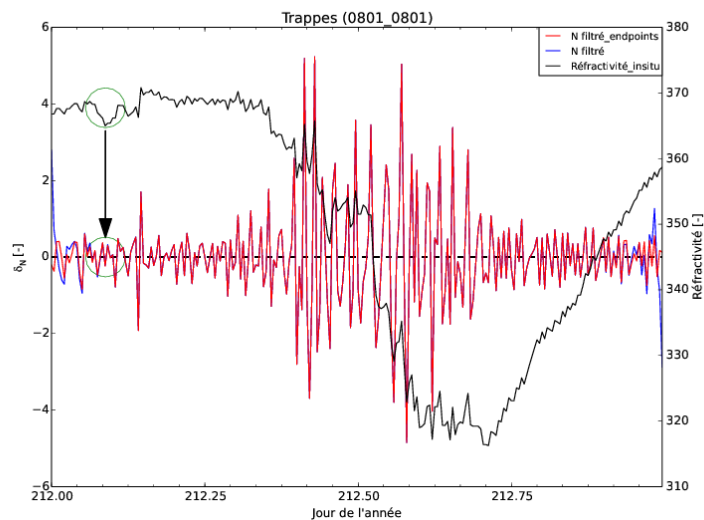


Fig. 2: Results of frequency filtering on in-situ refractivity measurements for Trappes AWS on August, 1st, 2013. Black curve represent the evolution of refractivity during 24h and red curve is the refractivity after the treatments. This figure highlights the interest of implementing the linear trend correction and the high-pass filtering process.

Treatments on AWS data

For this study, full datasets were needed. Considering the low missing data rate (0.2% to 1.9%), an algorithm was used in order to restore datasets. Linear interpolation is used as a standard treatment for these missing data. In order to treat outliers a median filter was used. Frequency filtering method using FFT with high-pass filter was applied on these complete datasets to keep only phenomena with less than 45min time period. Low frequency energy could affect our analysis so this high-pass filter was applied to avoid this perturbation.

The standard deviation of the refractivity variations was calculated over a sliding sample window of 2h. The width of the sample window was chosen to avoid taking into account the daily modulation of the signal.

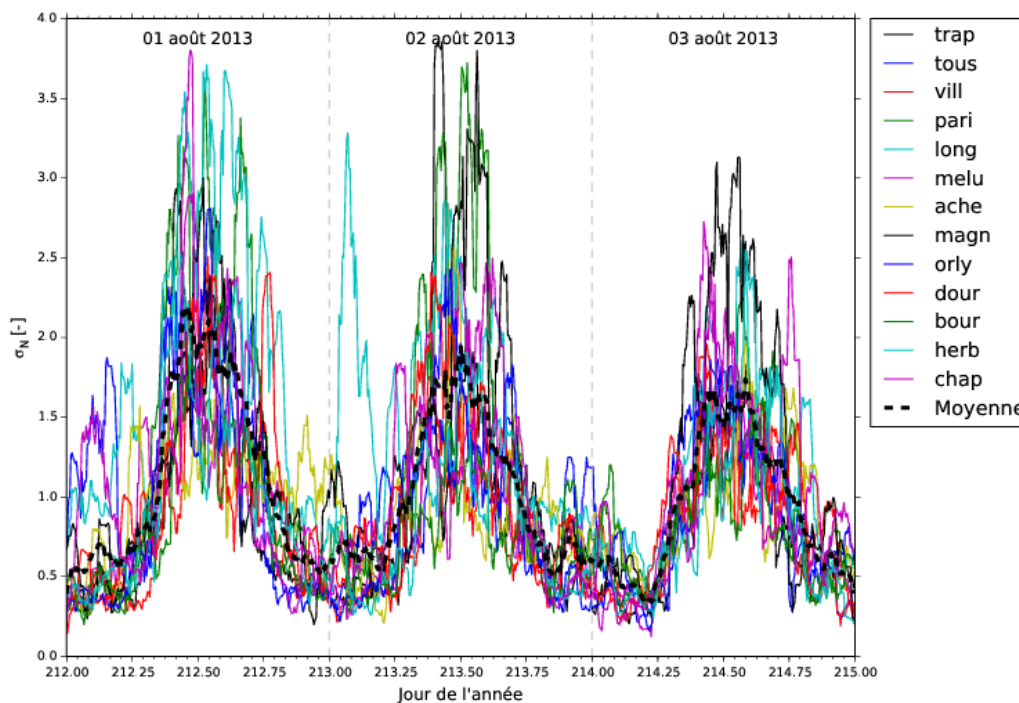


Fig. 3: Standard deviation (sliding sample window of 2h) for the 13 stations around Trappes radar from August, 1st to August, 3rd. Black dashed line represents the mean standard deviation value.

Treatments on radar data:

A first selection of known isolated targets was done in order to measure the refractivity variability around the radars. Ground echoes have to be isolated. If not the phase signal is a combination of several contributions of different targets and its analysis is much more complicated. This first selection was made based on observations of the echo power map combined with field observation. Fig. 1 shows different kinds of ground echoes identified with this method. Ground echoes are mainly caused by power line pylons, buildings, water towers, TV antenna. In most cases, these are very good targets for refractivity retrieval based on phase variations measurements.

As the first selection only represent a little percentage (less than 1%) of ground echoes available, a second selection was done. To select correct ground echoes allowing high-frequency refractivity retrieval a method was developed. Based on correlation between in-situ refractivity and radar refractivity this method allows to select ground echoes which are able to retrieve at least low-frequency refractivity signal. This treatment allows selecting more ground echoes so numerical statistical approach will be more significant on this sample.

4. Results

Standard deviation of in-situ refractivity signal

To characterize temporal refractivity variability, 2-h standard deviation of high passed signal of refractivity was used. This standard deviation computed on 13 AWS for a 1-year data set confirmed the observation of the previous study (Besson et al. 2011). This highlights fluctuations interpreted as turbulence due to daily heating from sunrise to the middle of the day. However the study of this index shows two important things:

- Mean level of night fluctuation during summer (0.4 refractivity units) is larger than during winter (0.2 refractivity units)
- High winter fluctuation level (0.6 refractivity units) is comparable to low summer fluctuation level (0.5 refractivity units)

In figure 3, temporal series of daily distribution of refractivity standard deviation show a strong seasonal modulation. These seasonal differences are coherent with turbulence level largely depending on daily insolation modulations.

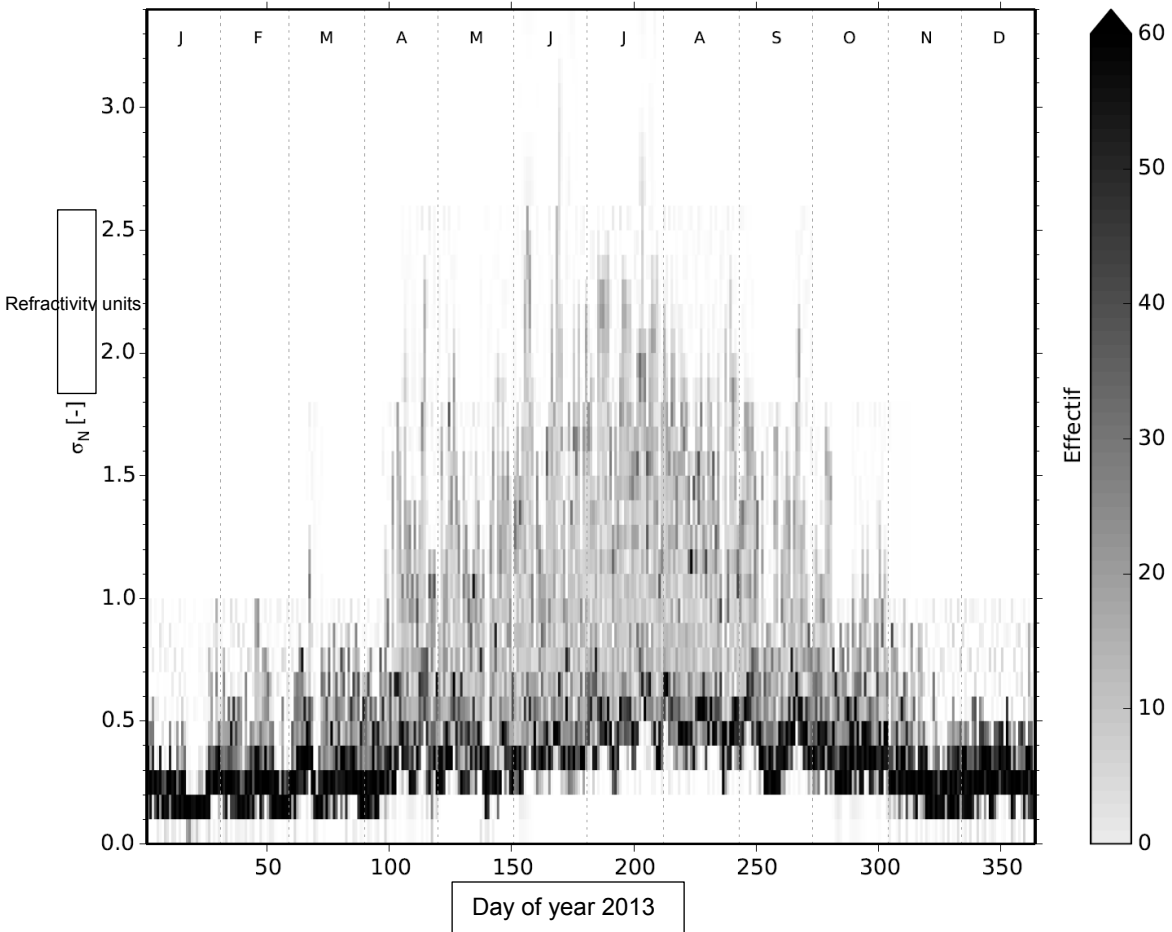


Fig. 4: temporal evolution of the daily distribution of refractivity standard deviation averaged over 13 AWS around Trappes radar for 2013. The size of the sampling window is 2h.

As expected, the variability of in-situ refractivity is more important than the variability of the radar refractivity. This can be explained by the integration realized for the calculation of radar refractivity (see above). Fig. 5 shows that the refractivity variability decreases with the integrated distance. In order to take this spatial integration into account and to compare in-situ measurements and radar measurements Taylor's hypothesis was applied to the AWS dataset. Using wind speed measurements at 10m, the temporal refractivity signal is propagated in one direction and the result is compared to radar refractivity retrieval.

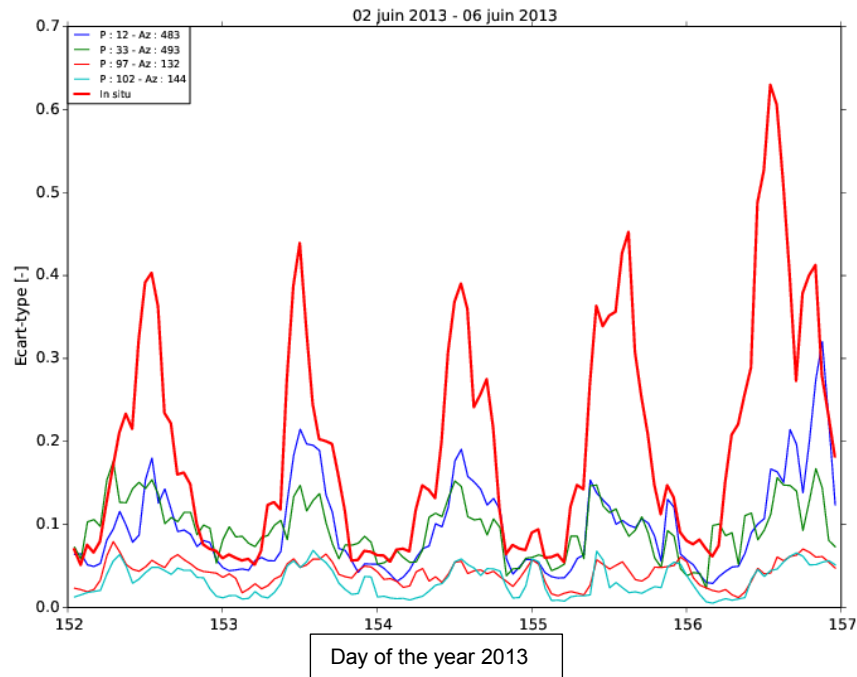


Fig. 5: Refractivity variations standard deviation (sampling window of 2h) function of the time from June, 2nd 2013 to June, 6th 2013. Thick red line: standard deviation for Trappes in-situ measurements. Blue line: Standard deviation for radar measurements (target at 2.9km) Green line: target at 7.9km Orange line: target at 23km and Cyan line: target at 24.5km

4. Perspectives

Further work will consist to look after statistical relations between the variability of the refractivity computes from AWS measurements with Taylors' hypothesis and radar retrieval variability of refractivity. Using data from SIRTA (Atmospheric research observatory based near Paris at 15km of Trappes) a turbulent parameter as Turbulent Kinetic Energy (TKE) will be compared to the standard deviation calculated during the study..

This work forms the basis for the preparation of a controlled condition measurement campaign. During this campaign, particular attention will be paid to the phase time derivate and spatial variations between artificial targets placed in the top of meteorological towers. Two radars will measure the signal from these targets and calculate the refractivity over several ranges by spatial differentiation.

5. References

Besson L, Boudjabi C, Caumont O, and Parent du Châtelet J, (2011): *Links between weather phenomena and characteristics of refractivity measured by precipitation radar. Bound.-Layer Meteor*

Boudjabi C, Parent du Châtelet J, (2009) *Evaluation of phase ambiguity problem due to sampling time when measuring refractivity with precipitation radar. In: 34th International conference on radar meteorology, Williamsburg, VA, USA. American Meteorological Society*

Fabry F., C. Frush, I. Zawadzki, A. Kilambi, 1997: *On the extraction of near-surface index of refraction using radar phase measurements from ground targets, J. Atmos. Ocean. Technol.*, 14:978-987.

Fabry F., 2004: *Meteorological value of ground target measurements by radar, J. Atmos. Ocean. Technol.*, 21:560-573.

Sherwood S.C., R. Roca, T.M. Weckwerth, and N.G. Andronova, 2010: *Tropospheric water vapor, convection, and climate. Reviews of Geophysics*, 48, RG2001.

Parent du Châtelet J, Boudjabi C, Besson L, and Caumont O, (2012): *Errors caused by long-term drifts of magnetron frequencies for refractivity measurement with a radar: Theoretical formulation and initial validation. J. Atmos. Oceanic Technol.*

Pielke R.A., 2001: *Influence of the spatial distribution of vegetation and soils on the prediction of cumulus Convective rainfall. Reviews of Geophysics*, 39, 151-177.